Ultrasonics 98 (2019) 15–19

Contents lists available at ScienceDirect

Ultrasonics

journal homepage: www.elsevier.com/locate/ultras

Generation of sub-microsecond quasi-unipolar pressure pulses

M.G. González[a,b,*], L.M. Riobó[a], L. Ciocci Brazzano[a,b], F.E. Veiras[a,b], P.A. Sorichetti[a], G.D. Santiago[a]

[a] Universidad de Buenos Aires, Facultad de Ingeniería, Grupo de Láser, Óptica de Materiales y Aplicaciones Electromagnéticas (GLOMAE), Paseo Colón 850, C1063ACV Buenos Aires, Argentina
[b] Consejo Nacional de Investigaciones Científicas y Técnicas, (CONICET), C1425FQB Buenos Aires, Argentina

ARTICLE INFO

Keywords:
Laser-generated ultrasound transmitters
Ultrasonic sensors
Piezoelectric polymer
Interferometry

ABSTRACT

We present a method to generate sub-microsecond quasi-unipolar pressure pulses. Our approach is based on the laser irradiation of a thin copper wire submerged in water. The acoustic waveforms were recorded using two different, well characterized, wideband detection techniques: piezoelectric and optical interferometry. The results show that the irradiated target behaves as an omnidirectional source. Moreover, the peak pulse pressure linearly depends on the laser fluence and the source size. From the results, we propose an empirical equation for the spatial and temporal profile of the pressure pulse. The method has several advantages: ease of implementation, high repeatability, wide ultrasonic bandwidth and quasi-unipolar time profile. These features lead to potential applications of this acoustic source in ultrasonic characterization such as transducer systems, materials or passive devices.

1. Introduction

Recent advances in imaging and biomedical applications of ultrasound technology are frequently based on time-domain techniques, using broadband pulses in the sub-microsecond range. This imposes stringent requirements on the characterization of sensors and the validation of signal processing algorithms, thus making necessary the use of highly repeatable, simple and efficient ultrasonic pulse sources.

The characterization of broadband sensors with quasi-unipolar pulses is of interest, since they mimic the response of many targets. An accurate characterization requires that the frequency spectrum of the short pulses extends to frequencies substantially lower than the low-frequency cutoff of the device under test. If this condition is met, the response of the sensor will be the same as that from a mathematically unipolar pulse (that is not physically achievable).

Different methods for pulse generation in liquids have been proposed, including electric discharges, collapse of bubbles [1] and irradiation with particle beams or electromagnetic radiation [2]. The advent of powerful pulsed laser sources opened the way to the development of a number of experimental schemes, with varying degrees of complexity [3–7].

Laser-induced ultrasound transmitters usually consist of optical absorbers, for efficient conversion of light energy into heat, surrounded by a medium with large thermal expansion coefficient. There are several works in the literature on laser-generated ultrasound transmitters, including mathematical modeling and analysis, effective absorbing materials, fiber-optic transmitters, and ultrasound beam focusing [8]. It is worth noting that metallic absorbers are among the most popular transmitters. Particularly, thin aluminum films and gold nanoparticles on a polydimethylsiloxane (PDMS) substrates are frequently used as metallic absorbers [8]. Moreover, the pressure generated by emitters based on gold nanoparticles are about three order of magnitude more efficient [8]. However, they are more difficult to implement.

Ultrasound generated by laser irradiation on metals, first proposed by White in 1963 [2], can be driven by ablation or thermoelastic effects. When the metallic target is immersed in a liquid, the generation of pressure pulses by bubble formation may play a dominant role [9]. The generation of pressure pulses by ablation of the target material requires high optical intensities. On the contrary, thermoelastic [8] and bubble formation [9] processes do not entail an irreversible alteration of the target, and take place with much lower intensities. Therefore they are more desirable in practical applications. For instance, a thin metal film irradiated by a short-pulsed laser beam is capable of inducing a broadband acoustic wave with high repeatability [10]. Of course, for efficient generation of high-frequency ultrasound, the properties of the medium surrounding the transmitter must be taken into account.

In this work we present experimental results on the generation of sub-microseconds ultrasonic pulses with high repeatability, using a

* Corresponding author.
E-mail address: mggonza@fi.uba.ar (M.G. González).

https://doi.org/10.1016/j.ultras.2019.05.002
Received 28 June 2018; Received in revised form 11 April 2019; Accepted 8 May 2019
Available online 23 May 2019

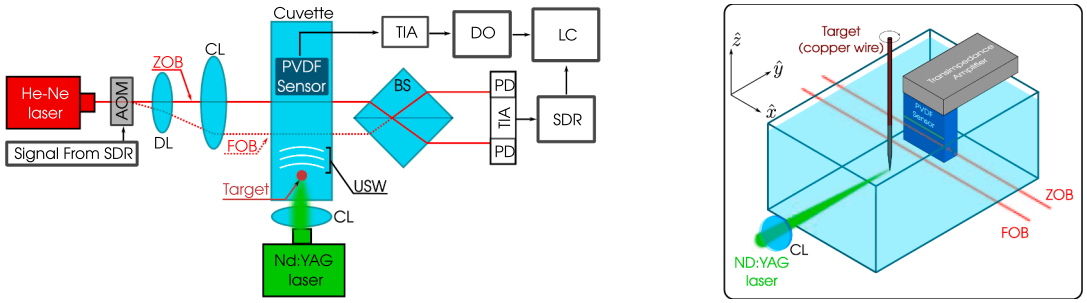

Fig. 1. Left: experimental setup used to characterized the method presented in this work. Right: Out-of-scale 3-D scheme of the cuvette. AOM: acousto-optic modulator. DL: diverging lens. ZOB: zero order beam. FOB: first order beam. CL: converging Lens. TIA: transimpedance amplifier. DO: digital oscilloscope. USW: ultrasonic waves. BS: beam splitter. SDR: software defined radio. PD: photodiode. LC: laptop computer.

small metallic wire as a target. Omnidirectional radiation of quasi-unipolar acoustic pulses is achieved by focusing nanosecond laser pulses on the tip of a thin (20–100 μm) copper wire submerged in water. The acoustic pulses were characterized by two different techniques: broadband piezoelectric transducers (using PVDF thin films) [11] and dynamic heterodyne interferometry [12]. The results from both techniques agree very well with each other. We also carried out simulations with a bubble generation model based on the Mie optical scatterig theory and classical and statistical nucleation theories [9]. Measurements and simulations show that the duration of the quasi-unipolar pressure pulse is close to that of the laser pulse. Interestingly, the quasi-unipolar pulses have an energy spectrum extending to very low frequencies. Furthermore, we propose a simple empirical equation to describe the scaling of the acoustic pulse amplitude with the optical fluence.

2. Materials and methods

The scheme of the experimental setup is presented in Fig. 1. The piezoelectric sensor and the metallic target used as the acoustic source, were both immersed in a large cuvette (120 mm × 80 mm × 55 mm) filled with deionized water. The size of the cuvette was chosen to avoid interference with the waves reflected from the walls of the cuvette, within the measurement time frame. The water temperature was measured with a calibrated thermocouple. This makes possible to determine the speed of sound in the water that surrounds the sensor. A frequency-doubled Nd:YAG laser (Continuum Minilite I, 532 nm, 5 ns, 10 Hz) and a converging lens were used to irradiate the target (copper wire). The lens focuses the laser beam on the copper wire, into a spot with a diameter close to that of the wire, thus providing a roughly spherical irradiated volume. The position in the cuvette of the source and the piezoelectric sensor position are adjusted using two XYZ translation stages. The sensor output was amplified with a transimpedance amplifier (EG&G Optoelectronics Judson PA-400), digitized by an oscilloscope (Tektronix TDS 2024, 2 GS/s, 200 MHz) and processed on a personal computer. The oscilloscope trigger signal was obtained from the laser Q-Switch pulse. The laser pulse energy was measured with a pyroelectric detector (Coherent LMP10).

Starting from a copper wire (diameter 100 μm), targets of different diameters were obtained by immersing the tip of the wire to a depth of 5 mm in ferric-chloride solution (as used for etching printed circuit boards) at room temperature during different times. After washing with deionized water and drying in air, the diameter of the targets were measured with an optical microscope.

The two polymeric piezoelectric sensors used in this work consist of a polyvinylidene fluoride (PVDF) film (25 μm of thickness) attached to an acrylic substrate with dimensions 30 mm × 30 mm × 10 mm. The active detection areas are 0.7 mm × 24 mm (line sensor) and 0.8 mm × 0.8 mm (quasi-point sensor). Given the experimental conditions in this work (distance from the source to the line sensor and sound propagation speed in water), the detector width (0.7 mm) can be neglected and, therefore, the line shape assumption is valid. The cut-off frequency of the piezoelectric detection system (sensor + amplifier) is 20 MHz (−3 dB). The transducers have a sensitivity of 100 μV/Pa and a noise equivalent pressure (NEP) of 2.2 mPa/$\sqrt{\text{Hz}}$ (line sensor) and 60 μV/Pa and 5.6 mPa/$\sqrt{\text{Hz}}$ (point sensor). Further details about the implementation and electric characterization can be found in [11].

The optical sensor was a heterodyne interferometer that uses a low-cost commercial software-defined radio (SDR) for optical modulation and demodulation. The detection scheme used in this work is the same system described in detail in [12]. A beam from a He-Ne laser source traverses an acousto-optic modulator (AOM) which is driven by a wideband power amplifier excited by a sinusoidal signal from the SDR (LimeSDR, [13]). This modulation produces a first-order diffracted beam (FOB) that has an optical frequency shift and propagates along with the zero-order undiffracted beam (ZOB). The beams are collimated and separated by a backward Galilean telescope (divergent lens, DL $f = -25$ mm, and convergent lens, CL $f = 200$ mm). In this way, the two parallel free beams (ZOB and FOB) enter the cuvette. The propagating pressure pulse alters the refractive index of the medium traversed by the optical beams, producing a variation of the optical path difference (i.e a phase modulation). In this way, the beams are used to sense the signal in different points within the medium. The beams are combined by a single element interferometer [14], producing two heterodyne interferograms in phase opposition. A balanced photodetector converts the optical fields into voltage signals which are processed by the SDR. The NEP of the optical system is 32 mPa/$\sqrt{\text{Hz}}$. It is worth noticing that in this experimental setup, both sensors satisfy the Fresnel condition for near field.

3. Integrating line sensors

Two of the sensors used in this work are of the integrating line type. In this context, integrating means that the detector size is larger than the size of the object. In this way, the received signal at a certain time is given by the instantaneous value of the integral of the acoustic field over the sensor area. Thereby, the shape of the detector strongly influences the temporal profile of the signal. We chose a linear shape because it can be easily implemented in both sensor technologies, piezoelectric and optical.

The response of an integrating sensor to a pressure pulse can be simulated by a parametric model described in a previous work [15]. In this model it is assumed that each point of the sensor surface behaves like a point detector that can be modeled as a linear, time invariant (LTI) system and the main characteristics of the sensors are introduced through transfer functions and/or filters applied to the LTI systems. Finally, the output signal is obtained from the integration of the responses of the LTI systems over the sensor surface. Fig. 2 presents the simulated responses of three sensors to a single positive pressure pulse from a spherical source of 25 μm radius in water. The source is assumed

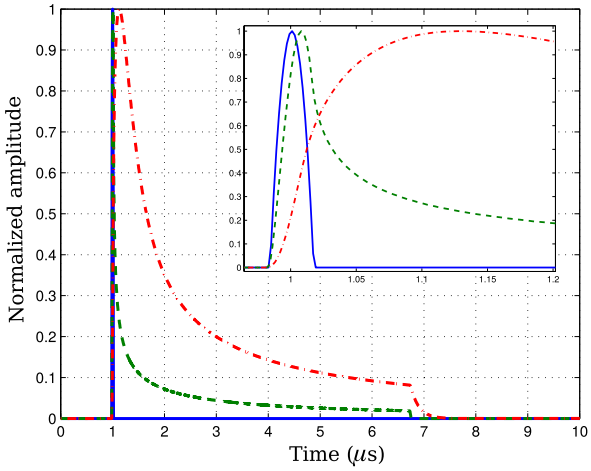

Fig. 2. Simulated response to a short duration positive pressure pulse. Solid line: ideal point sensor. Dashed and dash-dotted lines: integrating line sensors with bandwidth >10 MHz and <1 MHz, respectively. The inset shows a zoom of the simulation between 0.95 μs and 1.2 μs.

to be aligned with the center of the sensors and at a distance of 1.5 mm. The solid line represents the response of an ideal point sensor. The other two, belong to the integrating linear sensors (length 20 mm) with high (20 MHz) and low system bandwidths (1 MHz). These values correspond to the piezoelectric and optical sensors used in this work. It can be seen that the output signal from the line integrating sensors have longer duration than the one given by the ideal point detector (see inset in Fig. 2). The difference in bandwidth modifies the width and rise- and fall-times of the main peak.

The response to a bipolar pressure pulse generated by a spherical source with the same duration of the previous case is presented in Fig. 3. It may be seen that the response of the integrating sensor with large system bandwidth is quite similar to that of the ideal point sensor. The sensor with limited system bandwidth gives a significantly different output signal. Remarkably, the response to a bipolar pressure pulse of both integrating linear sensors are much shorter than for a unipolar pulse with the same duration. This was expected since the bipolar pulse has a very small energy content at low frequency.

4. Experimental results

We carried out measurements on the pulses generated by copper

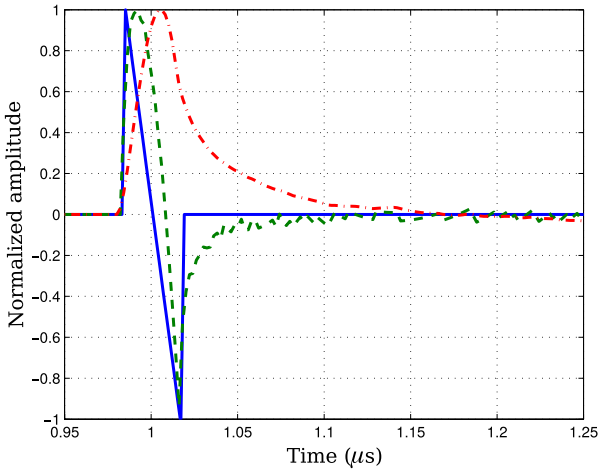

Fig. 3. Simulated response to a short duration bipole pressure pulse.Solid line: ideal point sensor. Dashed and dash-dotted lines: integrating line sensors with bandwidth >10 MHz and <1 MHz, respectively.

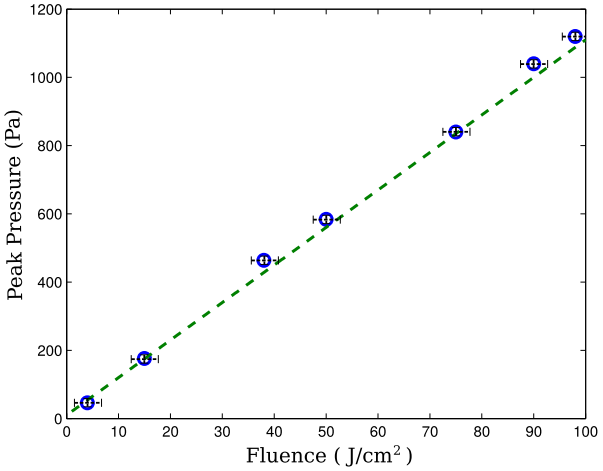

Fig. 4. Measured peak pressure vs. laser fluence. The distance between the source (copper wire of 50 μm of diameter) and the sensor was 5 mm.

targets with diameters between 20 and 100 μm. For each target we captured the pressure pulses generated with laser fluences between 0.01 and 100 J/cm^2. It is found that for each target diameter there is a fluence value, indicated as F_c, above which there is a sharp increased of the pulse amplitude. Measured values of F_c are in the range from 0.02 to 0.1 J/cm^2. Below F_c no discernible acoustic signals could be found above the background noise level. This behavior is consistent with the acoustic emission from the bubble formation process [9]. Under this assumption, to ensure bubble formation, we used fluences above 5 J/cm^2 in the remaining experiments in this work.

In the next set of measurements the dependence of the pressure on the laser fluence was determined. The plot on Fig. 4 shows the peak pulse pressure generated by a target with a diameter of 50 μm, irradiated with fluences between 5 and 100 J/cm^2, measured by a piezoelectric sensor. The results show a linear dependence between the peak pressure and the laser fluence. The same behavior was found for all the target diameters tested in this work (20–100 μm). The maximum peak pressure obtained with this method was 2.5 kPa, with a wire diameter of 100 μm and a fluence of 100 J/cm^2, measured with the sensor located at 5 mm from the source.

We studied the dependence of the peak pressure on the source size using the piezoelectric sensor. The laser spot size was in all cases matched to the target diameter. Moreover, the laser pulse energy was adjusted to keep the fluence on the target at the desired level. The plot in Fig. 5 presents the peak pressure for different copper target diameters and also shows a linear behavior.

Finally, for each target diameter and using the XYZ translation stages, we captured the pressure pulses at different relative positions between the source and the sensor. We found that the acoustic source has an omnidirectional behavior.

The time integral of the voltage signal from the piezoelectric sensor gives the time dependence of the pressure pulse captured by the transducer [15]. Two examples are given in Figs. 6 (line detector) and 7 (point detector). According to Section 3, the signals shapes are consistent with a quasi-unipolar positive pulse recorded by a sensor with a high frequency cutoff of 20 MHz, and low frequency cutoff about 100 Hz (limited by the detection system). As shown in Fig. 3, we would expect that a bipolar pulse sensed by a line sensor would give rise to a sensibly shorter response. Instead, we observed a longer response corresponding to a unipolar pulse that exhibits frequencies components substantially lower than the low-frequency cutoff of the transducer (Fig. 2). It must be remarked that the small oscillations superimposed to the signal after the main peak are due to the reflections of the acoustic waves on the lateral boundaries of the PVDF film [15].

Fig. 8 presents the pressure signal recorded by the optical sensor. In the experimental setup shown in Fig. 1, the zero-order (ZOB) and first-

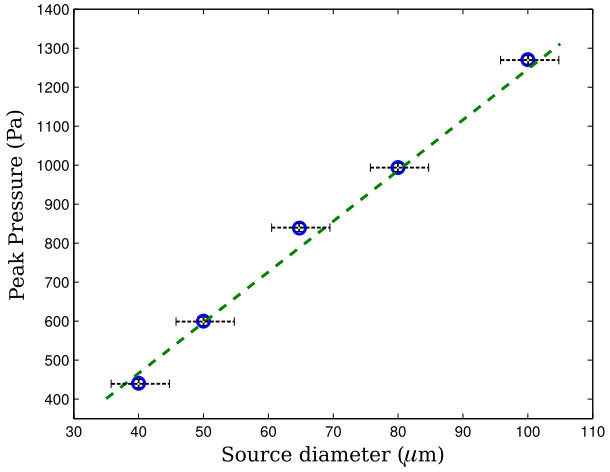

Fig. 5. Measured peak pressure vs acoustic source diameter. The distance between the source and the sensor was 8 mm and the laser fluence on the target was kept constant at ~50 J/cm^2.

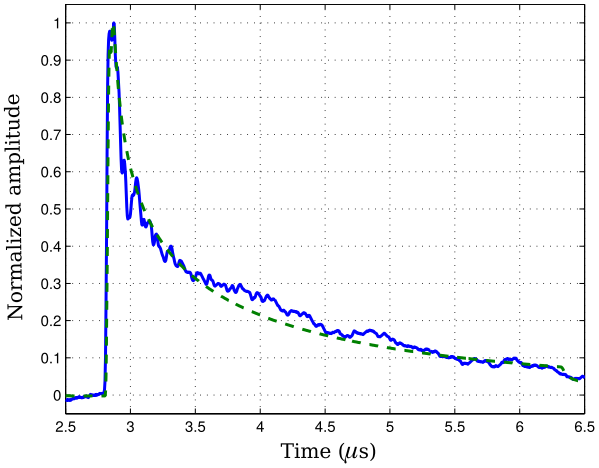

Fig. 6. Measured (solid line) and simulated (dashed line) pressure recorded by the piezoelectric line sensor. The distance between the source (50 μm) and the sensor was 4.2 mm.

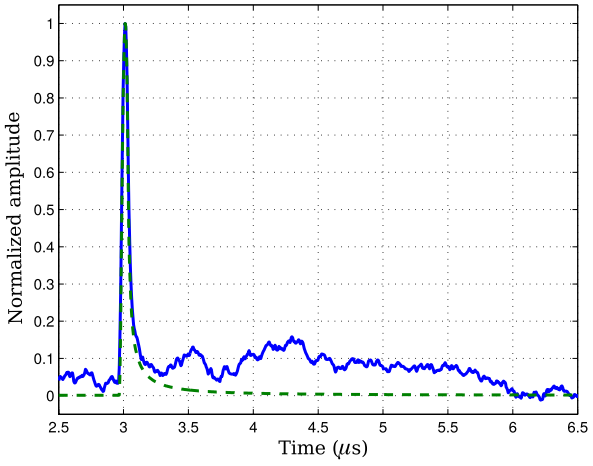

Fig. 7. Measured (solid line) and simulated (dashed line) pressure recorded by the piezoelectric quasi-point sensor. The distance between the source (50 μm) and the sensor was 4.5 mm.

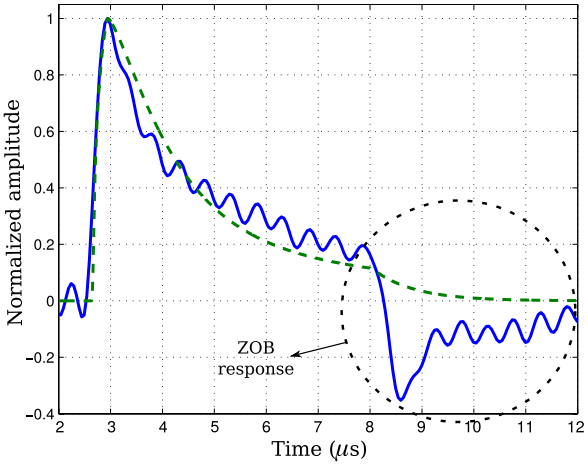

Fig. 8. Measured (solid line) and simulated (dashed line) pressure recorded by the optical sensor. The first (main) peak corresponds to the FOB. The distance between the source (50 μm) and the sensor was 4 mm.

order (FOB) beams will sense the pressure pulse in two different regions in the sample. The information from the acoustic signal is recovered from the phase difference $\Delta\phi(t)$ between the two beams, at the exit plane of the cuvette. This phase difference depends on the integrated effects of the refractive index variations along the propagation paths in the cuvette, $n_{i0}(t)$ (ZOB) and $n_{i1}(t)$ (FOB) [12]. Therefore,

$$\Delta\phi(t) = \frac{2\pi}{\lambda} L\,[n_{i1}(t) - n_{i0}(t)] \tag{1}$$

where L is the geometrical length of the propagation path within the medium in the cuvette. In our experiment, we assume that the medium is acoustically non-dispersive in the frequency range of interest. Thus, the time dependence of the integrated refractive index variation of the FOB and ZOB are related by

$$n_{i0}(t) = \alpha\, n_{i1}(t - \Delta t) \tag{2}$$

where α is an attenuation constant and Δt is a time delay that depends on the geometric distance between the beams and the speed of sound in the medium. Consequently, two proportional and time delayed responses with opposite signs are generated within the interferograms. In Eq. (2), it is assumed that the pressure pulse reaches the modulated beam (FOB) first, as it is clear from Fig. 1. From the parameters of the optical setup and the medium, it follows that the temporal resolution of the measurements is about 0.4 μs (i.e a bandwidth < 1 MHz) [12]. It must be noted that, the oscillations superimposed on the signal, are an artifact due to the finite-size window used for the Fast Fourier Transform.

In addition, we used a set of converging lenses to reduce the diameter of the optical waist of the HeNe laser beams in the cuvette. In this way, as expected [16], we increased the high frequency response of the system up to 15 MHz. Fig. 9 shows the signal captured with improved bandwidth together with the previous one. It can be seen that the new temporal profile is similar to that obtained with the piezoelectric detector (Fig. 6).

As mentioned above, the ultrasound generation would be driven by the bubble formation effect taking place in the liquid surrounding the irradiated metallic target. We carried out simulations using a modified version of the model described in [9]. This model is based on the Mie optical scattering theory, and the classical and statistical nucleation theories. The time evolution of the acoustic pressure field is determined by the bubble radius (R_b). The pressure signal at the position r and time t is given by the equation

$$p(r,\,t) \propto \frac{R_b(t_r)}{r}\left[(P_L(t_r) - P_0) + \frac{1}{2}\rho_L \dot{R}_b{}^2\right] \tag{3}$$

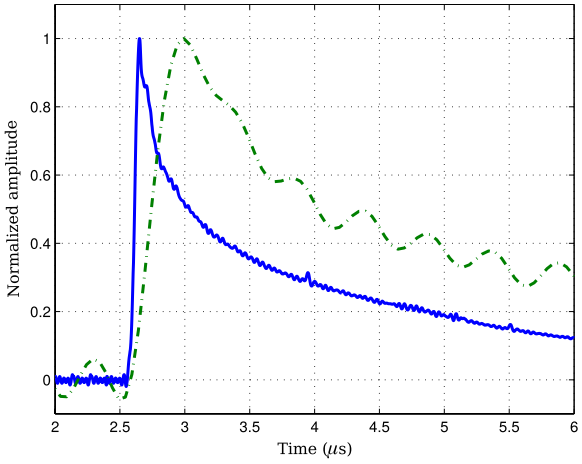

Fig. 9. Comparison between the measured pressure recorded by the optical sensor with a large waist (dashed-dot line) and with a reduced waist; improved bandwidth (solid line). The distance between the source (50 μm) and the sensor was 4 mm.

where $t_r = t - r/c$, c is the sound speed in water, P_L and ρ_L are the pressure and density of water on the bubble surface, and P_0 the water equilibrium pressure, and the source bubble is located at the coordinate origin. The input parameters of the model are the thermal boundary conductance between copper and water (50 MW/km^2), the target diameter (supposed of spherical shape), the duration (5 ns) and intensity of the laser pulse, the wavelength (532 nm), and the ambient temperature (300 K). The main modification made on the model is that he heating originated by a short laser pulse is significant only on the surface of the metallic target (< 1 μm), as shown experimentally and analytically by White [2]. The simulations were carried out using a program developed in GNU/Octave. The thermodynamic properties of water as a function of temperature and density were calculated according to the tables from the International Association for the Properties of Water and Steam (IAPWS, 2009), and the thermal transport and optical properties of copper were obtained from references [17,18], respectively.

The main results found from the simulations are: (i) for fluences greater than $5F_c$, there is a linear dependence between p and F; (ii) the irradiated surface of the copper target can reach a temperature up to 1400 K, (iii) the duration of the pressure pulse is close to that of the laser pulse, (iv) the temporal shape of $R_b(t)$ can be fitted by a quadratic equation, and (v) for target sizes greater than 1 μm, $p(t)$ and $R_b(t)$ follow the same general trend.

In summary, we found that: (a) the irradiated copper target behaves as an omnidirectional acoustical source; (b) for each laser pulse, the source generates a single quasi-unipolar positive pressure pulse and (c) the peak amplitude of the acoustic pulse has a linear dependence on laser fluence and the target diameter. Based on these results, we propose a simple empirical equation to represent the time (t) and spatial ($\mathbf{r}$) dependence of the pressure signal generated at $t = 0$ s by a laser pulse of fluence F on a copper target of radius a located at $\mathbf{r}_a$:

$$p(\mathbf{r}, t) \propto F \frac{a^2 - (|\mathbf{r} - \mathbf{r}_a| - ct)^2}{2a\ |\mathbf{r} - \mathbf{r}_a|} H(a - ||\mathbf{r} - \mathbf{r}_a| - ct|) \quad (4)$$

where H is the Heaviside function. Even though this expression describes a non physical unipolar pulse, is a valid approximation if the signal acquisition time span is short in comparison to the reciprocal of the lower cutoff frequency of the detection system. This condition is met in all the pulses measurements presented in this work.

In Figs. 6–8 the green dashed line represents the convolution of the sensor response with the acoustic pressure signal given by Eq. (4). The agreement with the experimental data is quite good. Moreover, taking into account the sensor transfer function [15], the acoustic bandwidths of the pressure pulses were in the range between 10 and 50 MHz (as explained above, the low frequency cutoff of the system is about 100 Hz).

5. Conclusions

In this work, we present a method to generate sub-microsecond quasi-unipolar pressure pulses. It is based on the generation of ultrasonic waves by laser radiation of a thin copper wire (20–100 μm diameter). Irradiating with visible laser pulses (5 ns FWHM), we achieved acoustic pulses up to 2.5 kPa peak amplitude and 50 MHz bandwidth. The acoustic signals were captured by optical and piezoelectric (point and line) detectors. The low frequency cutoff of the detection system was around 100 Hz, and the signal acquisition time span was of about 10 μs. Experimental data show that the irradiated target behaves as an omnidirectional source of quasi-unipolar acoustic pulses. Copper has several advantages as target material to generate acoustic pulses by irradiation. Moreover, the diameter of the copper wire can be easily controlled through chemical etching.

From our measurements, together with simulations results from a bubble model of acoustic emission, we propose a simple empirical equation that gives a very good fit of the spatial and temporal profile of the measured pressure pulse.

The method is easy to implement and provides highly repeatable, wideband quasi-unipolar ultrasonic pulses. These advantages lead to potential applications of this acoustic source as a reference for the characterization of ultrasonic transducer systems and components.

Acknowledgements

This work was supported by the University of Buenos Aires (grants UBACyT 20020160100052BA, 20020160100042BA, 20020170200232BA) and ANPCyT, grant PICT 2016–2204.

References

[1] H. von S. Fluegge, Handbuch der Physik, Band XI/2: Akustik II, Springer-Verlag, Berlin, Germany, 1962.
[2] R.M. White, Generation of elastic waves by transient surface heating, J. Appl. Phys. 34 (1963) 3559–3567.
[3] C. Scruby, R. Dewhurst, D. Hutchins, S. Palmer, Quantitative studies of thermally generated elastic waves in laser-irradiated metals, J. Appl. Phys. 51 (12) (1980) 6210–6216.
[4] S. Davies, C. Edwards, G. Taylor, S. Palmer, Laser-generated ultrasound: its properties, mechanisms and multifarious applications, J. Phys. D 26 (1993) 329–348.
[5] E. Biagi, F. Margheri, D. Menichelli, Efficient laser-ultrasound generation by using heavily absorbing films as targets, IEEE Trans. Ultrason., Ferroelect., Freq. Contr. 48 (2001) 1669–1680.
[6] V. Kozhushko, P. Hess, Laser-induced focused ultrasound for nondestructive testing and evaluation, J. Appl. Phys. 103 (2008) 124902.
[7] W. Chan, T. Hies, C. Ohl, Laser-generated focused ultrasound for arbitrary waveforms, Appl. Phys. Lett. 109 (2016) 174102.
[8] S. Chen, Review of laser-generated ultrasound transmitters and their applications to all-optical ultrasound transducers and imaging, Appl. Sci. 25 (2017) 1–22.
[9] E. Acosta, M.G. Gonzalez, P. Sorichetti, G. Santiago, Laser-induced bubble generation on a gold nanoparticle: a nonsymmetrical description, Phys. Rev. E 92 (2015) 062301.
[10] W. Chan, T. Hies, C. Ohl, Thermoelastic response of thin metal films and their adjacent materials, Appl. Phys. Lett. 102 (2013) 021908.
[11] A. Abadi, L.C. Brazzano, P. Sorichetti, M.G. Gonzalez, Integrating line piezoelectric sensor for optoacoustic tomography: implementation and electrical characterization, Revista Elektron 1 (2) (2017) 53–57.
[12] L. Riobo, F. Veiras, M. Garea, P. Sorichetti, Software defined optoelectronics: space and frequency diversity in heterodyne interferometry, Sensors (2018).
[13] LimeMicrosystems, <http://myriadrf.org/projects/limesdr/>, limeSDR.
[14] J. Ferrari, E. Frins, Single-element interferometer, Opt. Comm. 279 (2) (2007) 235–239.
[15] A.F. Vidal, L.C. Brazzano, C. Matteo, P. Sorichetti, M.G. Gonzalez, Parametric modeling of wideband piezoelectric polymer sensors: design for optoacoustic applications, Rev. Sci. Instrum. 88 (9) (2017) 095004.
[16] G. Paltauf, R. Nuster, M. Haltmeier, P. Burgholzer, Photoacoustic tomography using a mach-zehnder interferometer as an acoustic line detector, Appl. Opt. 46 (16) (2007) 3352–3358.
[17] T.Q. Vo, B. Kim, Interface thermal resistance between liquid water and various metallic surfaces, Int. J. Precis. Eng. Manuf. 16 (7) (2015) 1341–1346.
[18] I. Lisiecki, F. Billoudet, M. Pileni, Control of the shape and the size of copper metallic particles, J. Phys. Chem. 100 (1996) 4160–4166.